

1 Article

2 Modelling, parameters identification and 3 experimental validation of a lead acid battery bank 4 using genetic algorithms

5 H. Eduardo Ariza ¹, Edison Banguero², Antonio Correcher ³, Ángel Pérez-Navarro⁴ and Francisco
6 Morant⁵

7 ¹ Grupo de Investigación en Sistemas Inteligentes, Corporación Universitaria Comfacaucua, Popayán CP
8 190003, Colombia; helarcha@upv.es

9 ² Instituto de Automática e Informática Industrial-ai2, Universitat Politècnica de València, Valencia, CP
10 46022, Spain; edbanpa@doctor.upv.es (E.B); ancorsal@upv.es (A.C.); fmorant@upv.es (F.M.);

11 ³ Instituto Universitario de Ingeniería Energética - IUIIE, Universitat Politècnica de València, Valencia, CP
12 46022, Spain; anavarro@iie.upv.es (A.N.)

13 * Correspondence: helarcha@posgrado.upv.es; Tel +57-2838-6000

14

15

16 **Abstract:** Accurate and efficient battery modeling is essential to maximize the performance of
17 isolated energy systems and to extend battery lifetime. This paper proposes a battery model that
18 represents the charging and discharging process of a lead-acid battery bank. This model is
19 validated over real measures taken from a battery bank installed in a research center placed at “El
20 Chocó”, Colombia. In order to fit the model, three optimization algorithms (Particle Swarm
21 Optimization, Cuckoo Search, and Particle Swarm Optimization+Perturbation) are implemented
22 and compared, being the last one a new proposal. This research shows that the model with the
23 proposed algorithm is able to estimate and manage the real battery characteristics as SOC and
24 charging/discharging voltage. The comparison between simulations and real measures shows that
25 the model is able to absorb reading problems, signal delays, and scaling errors. The approach we
26 present can be implemented in other types of batteries especially those used in stand-alone
27 systems.

28 **Keywords:** Modelling; lead-acid battery; parameter identification; genetic algorithms;
29 experimental validation.

30

31 1. Introduction

32 The energy storage system most often used is battery technology [1]–[5]. Batteries are used as
33 power source for electric vehicles (EV), communication systems, electrical and electronic devices,
34 renewable energy systems (RES), etc. In RES such as stand-alone photovoltaic and wind power, the
35 battery type commonly used is lead acid battery due to their maturity and low cost [6]. These
36 batteries are composed of two-volt elements that connect in series and provide voltages of 12V, 24V,
37 48V, etc. However, lead acid batteries have a high impact on the lifetime costs of stand-alone
38 power-supply systems [6]. Some studies [7,8] reveal that batteries may account for up to 40% of the
39 overall system cost over its lifetime.

40 Accurate and efficient battery modeling is essential to maximize the performance of a system
41 and its battery lifetime. However, due to its non-linear nature [9] the battery charging and
42 discharging process is complex to be accurately modeled. Moreover, many aging phenomena take
43 place inside the battery during its life cycle such as corrosion, gassing effect, self-discharging,
44 diffusion process, etc. [10]. Different models have been developed and implemented to capture the
45 battery performance for various purposes [11]–[15]. Nevertheless, in order to effectively use a
46 specific mathematical model to a real system, highly accurate modeling and low computational time

47 are required [16]; therefore a parameters number must be tuned in order to accurately represent the
48 system working. Because system working depends on a high number of variable factors such as
49 environmental variables, life cycle, or type of facility, among others, some method has to be applied
50 to tune the model parameters.

51 Different methods have been proposed in the literature to identify the battery parameters [17]–
52 [20]. However, genetic algorithms (GA) have shown great performance. GA is a technique for
53 stochastic search, learning, and optimization [21]. GAs work on a set of potential solutions called
54 population. This population is composed of a series of solution known as individuals. The
55 individuals are formed by a series of positions that represent the variables called chromosomes. GA
56 has wide applications in bioinformatics, engineering, physics, computational science, mathematics,
57 and other related fields [22]–[26]

58 Regarding the optimization of hybrid energy system with battery PSO is considered as one of
59 the most used GA due to its good performance, flexibility, and simplicity [27]. Previous studies
60 show that this algorithm is used in the electrochemical model parameter identification of a li-ion
61 battery for automotive applications [28]–[32]. While the application of GA for the parameter
62 identification of lead acid batteries as those used in RES research is scarce, e.g., Guasch et al. [33]
63 used the battery model proposed by [34] and they added two extra parameters: level of energy and
64 state of health. These new parameters are able to predict the degradation of the battery capacity and
65 the increase of self-discharge current in the long time. In order to fit the model, they applied a
66 Levenberg–Marquardt algorithm to achieve a mean voltage error around 1%. Besides to the 21
67 parameters identified in [34], Blaifi et al. [35]–[37] propose an improvement of 4 parameters for the
68 estimation approximately of the gassing and the saturation levels. The simulation results shows that
69 mean error with parameters given by [34] was 1.49%. While the mean error with parameters
70 identification by GA was 0.45%. However, one disadvantage of the model is the high calculation
71 time due to the large number of samples required for a good identification.

72 Another very attractive GA that can be used in the parameters identification is Cuckoo Search
73 (CS) [38, 39]. In this genetic algorithm, the random walk is generated via Lévy flights as search
74 strategy. CS is considered as a modern meta-heuristic algorithm able to solve complex optimization
75 problems with high accuracy [40]–[42].

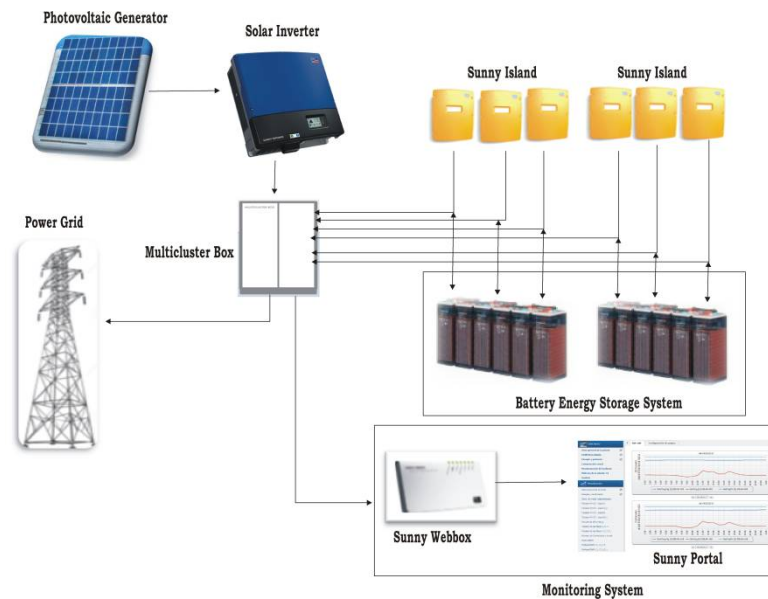
76 Taking into account the above-mentioned, this paper explores the use of GA to fit a
77 mathematical model of batteries in order to represent the real working of a research center. This
78 research has chosen the model developed by [34] because of its ability to cope with a widest range of
79 lead acid batteries. Additionally, three GA (PSO, PSO+Perturbation, and CS) are implemented and
80 compared to identify the parameters of a lead acid OPzS type battery bank. Where, we present
81 PSO+Perturbation GA as a new proposal for the parameters identification. Moreover, four new
82 parameters are added to the Copetti model. These parameters allow a better adjustment of the
83 curves of charging/discharging voltage of the acid lead battery. Equivalent circuit models and GAs
84 are simulated on LabView. The simulation results are validated with experimental data obtained
85 from a research center “Centro de Investigación en Energías Renovables del Departamento del
86 Chocó (Colombia) – CIERCHOCÓ.

87 This paper is organized as follows. In Section 2, a system description of the research center is
88 presented. In Section 3 presents the battery model, the parameters proposed by Copetti and the
89 addition of four new parameters to the model. Section 4 describes the GAs and their
90 implementation. The results obtained are presented in Section 5. Finally, the conclusions are
91 presented in Section 6.

92 2. Experimental system in CIERCHOCÓ

93 The real battery energy storage system (BESS) is composed of 48 TECHNO SUN
94 2V-OPzS-TCH2765 electrochemical accumulators divided into two branches of 24 cells connected in
95 series. According to the manufacturer’s characteristics, a single cell provides: nominal capacity 2770
96 Ah (C120). Additionally, the building integrates a photovoltaic (BIPV) system (see Figure 1). It is
97 composed of 80 polycrystalline silicon modules (Amerisolar ASP-6P30; 250 W each one), a 20 kW

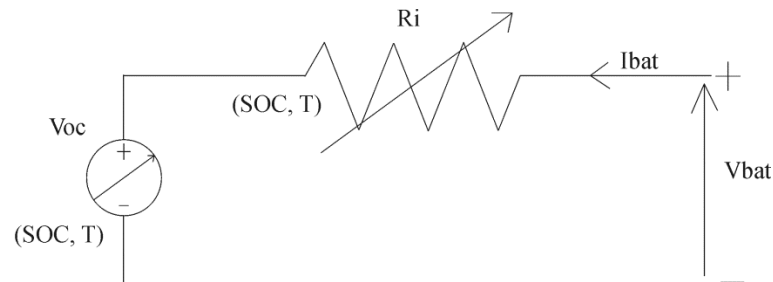
98 (STP 20000TL-30; SMA) DC/AC inverter, a multicluster box (220V, 60Hz), and 6 sunny island ac/dc
 99 chargers inverters. Moreover, a data acquisition system stores data every 15 minutes.
 100



101
 102 **Figure 1.** Block diagram of the BIPV system

103 3. Battery model test

104 The Copetti's model describes four operation modes for the battery system: a charging zone, a
 105 discharging zone, an overcharging zone and an intermediate zone representing a soft transition
 106 between charging/discharging modes [43]. Moreover, this model is based on a simple resistor model
 107 (see Figure 2) that is composed of an open circuit voltage source (V_{oc}) based on the batteries state of
 108 charge (SOC), and a resistor R dependent on current (I_{bat}), temperature (T) and SOC [34], [44], [45].



109
 110 **Figure 2.** Equivalent circuit battery model.

111 According to Figure 2, V_{bat} is given by equation (1):

112

$$V_{bat} = V_{oc} \pm I_{bat}R_i \quad (1)$$

113 where, I_{bat} is the current circulating through battery. $I_{bat} < 0$ during charge and $I_{bat} > 0$ during
 114 discharge.

115 The discharge voltage is simulated through equation (2), while the charge voltage is simulated
 116 with equation (3). Where, n_s are the electrochemical accumulator's number, and ΔT is the
 117 temperature variation.
 118

$$V_{dc}(t) = n_s [V_{bodc} - K_{bodc}(1 - SOC(t))] - n_s \frac{|I_{bat}(t)|}{C_{10} * k_{c10dc}} \left(\frac{P_{1dc}}{1 + |I_{bat}(t)|^{P_{2dc}}} + \frac{P_{3dc}}{SOC(t)^{P_{4dc}}} + P_{5dc} \right) * (1 - \alpha_{rdc} \Delta T(t)) \quad (2)$$

119

$$V_c(t) = n_s(V_{boc} + K_{boc}SOC(t)) + n_s \frac{I_{bat}(t)}{C_{120} * k_{c120c}} \left(\frac{P_{1c}}{1 + I_{bat}(t)^{P_{2c}}} + \frac{P_{3c}}{(1 - SOC(t))^{P_{4c}}} + P_{5c} \right) * (1 - \alpha_{rc}\Delta T(t)) \quad (3)$$

120

$$\Delta T = T - T_{ref} \quad (4)$$

121 The reference temperature (T_{ref}) is 25 °C. The terms P_{1dc} , P_{2dc} , P_{3dc} , P_{4dc} , and P_{5dc} are losses
 122 associated with the internal resistance as a function of the duty point [33], while the terms P_{1c} , P_{2c} , P_{3c} ,
 123 P_{4c} , and P_{5c} are charge parameters. The terms V_{boc} is the remaining voltage when the battery is
 124 discharged, K_{boc} and K_{bdc} relates the open circuit voltage of the battery with its SOC in the discharge
 125 and charge cycles respectively. K_{c120c} is a gain associated with battery capacity. α_{rdc} and α_{rc} provides
 126 the relationship with temperature [33].

127 The SOC is understood as the fraction or percentage of the capacity is still available in the
 128 battery and is estimated by equation (5). SOC_o corresponds to the battery initial SOC and C_{bat} is
 129 battery capacity in Ah.

$$SOC(t) = SOC_o - \int_0^t \frac{I_{bat}(t)}{C_{bat}} dt \quad (5)$$

130 where, $0 \leq SOC(t) \leq 1$. Equation (5) discrete implementation is:

131

$$SOC(t+1) = k_{soc} * \left[k_l * \Delta(t) \left(\frac{I(t+1) - I(t)}{2} + I(t) \right) * \frac{1 * k_{c_bat}}{C_{bat}} \right] \quad (6)$$

132 where k_{soc} is an overall gain of SOC; k_l is related to coulomb efficiency; Δt is the sampling period;
 133 and k_{c_bat} is an associated parameter to battery aging. New parameters (k_{c120} , k_{soc} , k_l , k_{c_bat}) have an
 134 initial value of 1 to maintain the original model performance.

135 Table 1, compares the parameters identified by [34] with the values published by [33] and [35]–
 136 [37] showing a high dispersion between the different authors.

137

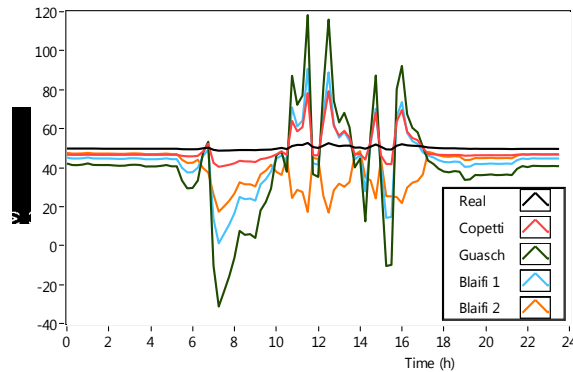
Table 1. Nominal values of the identified parameters by some authors.

Parameters	Guasch [33]	Copetti [34]	Blaifi [35], [36]	Blaifi [37]
V_{boc} (V)	2.147	2.085	2.148	2.1612
K_{boc} (V)	0.284	0.12	0.127	0.219
P_{1dc} (VAh)	4.083	4	0.406	9.5044
P_{2dc}	-6.634	1.3	3.041	4.9361
P_{3dc} (Vh)	0.27	0.27	1.218	0.9311
P_{4dc}	1.5	1.5	0.7812	0.037
P_{5dc} (Vh)	0.02	0.02	0.484	1.8837
α_{rdc} (°C ⁻¹)	0.007	0.007	0.0197	0.0167
V_{boc} (V)	1.98	2	1.781	1.9016
K_{boc} (V)	0.149	0.16	0.5313	0.16
P_{1c} (VAh)	5.923	6	7.234	6.0809
P_{2c}	0.024	0.86	0.667	1.6701
P_{3c} (Vh)	0.48	0.48	0.078	0.3375
P_{4c}	1.2	1.2	0.492	0.9853
P_{5c} (Vh)	0.036	0.036	0.7421	1.7838
α_{rc} (°C ⁻¹)	0.025	0.025	0.43	0.01

138

139 The model is able to choose the discharging equation when the input signal has a positive sign
 140 (+A); otherwise, the model chooses the charging equations if the current sign is negative (-A).
 141 Current and temperature are taken as input signals.

142 Figure 3 shows a comparison between the experimental system performance and the battery
 143 model using parameter sets from Table 1. Furthermore, Table 2 presents the mean errors obtained
 144 by simulation with parameters reported in [33]–[37]. In the Table 2 it is observed that with the
 145 parameters reported by [34] it obtains the lowest mean error.



146

147 **Figure 3.** Model test using the parameters published in Table 1.

148

Table 2. Mean error using the parameters reported in the literature.

Mean error (%)	Charge voltage	Discharge voltage
[33]	40.06	37.91
[34]	16.93	7.79
[35], [36]	20.98	22.16
[37]	42.10	14.00

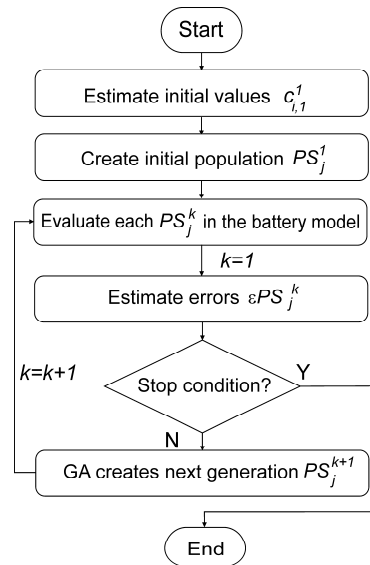
149

150 In the simulation of battery voltage, it is observed that this model represents the battery
 151 dynamics but with different scales and time delays. Therefore, the battery model must be used to fit
 152 the real battery dynamics.

153 4. Parameter identification

154 Due to the nonlinearity and complexity of the battery model, this proposal uses GA to find one
 155 possible optimal solution that belongs to a Pareto's front. Parameter identification was carried out
 156 in the same conditions with different GA in order to compare the algorithms. The general
 157 identification process for all GA is shown in **Error! Reference source not found.**, it starts with the
 158 estimation of initial coefficients values that are grouped in a parameter set (*PS*), in the second step,
 159 the initial *PS* is used to creates a random population of size *j*. In the third step, each single *PS* is
 160 evaluated into the model using inputs signals taken of real system. In the fourth step, the simulated
 161 outputs are compared with real outputs to estimate the *PS error*. Next, if the stop condition is
 162 fulfilled the process ends, otherwise, the GA creates a new population using specific criteria and
 163 back to the fourth step for a second iteration. The stop condition could be a defined iterations
 164 number or get an error lowest that a defined umbral.

165



166

167

Figure 4. Global identification process algorithm

168

169

170

171

172

The model describes both charging and discharging processes with different equations. The input current signal may change from positive sign (discharge) to negative sign (charge) several times in the same simulation, then the identification a PS that represents the real BESS with accuracy, requires the identification of one PS for each working mode. Therefore, a particular PS in the battery model consists of:

$$PS = \begin{cases} I(A) < 0; & PS = \{V_{boc}, K_{boc}, P_{1c}, P_{2c}, P_{3c}, P_{4c}, P_{5c}, \alpha_{rc}, k_{c120c}, k_{socc}, k_{lc}, k_{c_batc}\} \\ I(A) \geq 0; & PS = \{V_{bodc}, K_{bodc}, P_{1dc}, P_{2dc}, P_{3dc}, P_{4dc}, P_{dc}, \alpha_{rdc}, k_{c120dc}, k_{socdc}, k_{ldc}, k_{c_batdc}\} \end{cases}$$

173

A general PS is defined as:

$$PS_j^k = \{c_{1,j}^k, c_{2,j}^k, c_{3,j}^k, \dots, c_{i,j}^k\}$$

174

175

176

where $c_{i,j}^k$ represents any parameter of the PS ; e.g, $c_{1,2}^8$ is the value of first parameter (V_{bo}) in second parameter set of the 8th population PS_{28} . This parameter involve both V_{boc} and V_{bodc} .

177

178

In the first step, the initial values coefficients were taken from literature (Table 1). In the second step, the initial population ($k=1$) of size j is an array of PS that is creates following the bellow rules:

$$PS_j^1 = \begin{cases} j=1; & c_{i,1}^1 = c_{i,1}^1 \\ j \geq 1; & c_{i,j}^1 = (c_{i,j}^1 \cdot z \cdot v_d) + c_{i,j}^1 \end{cases}$$

179

180

181

182

183

$j=1$ ensure that the first population keeps the initial coefficients. For $j \geq 1$, the coefficients values change in a random way, where z represents a is random number ($z \in [-1, 1]$) and v_d is a value which generates a possible dispersion of the parameters $c_{i,j}^1$ in the initial population such that $c_{i,j}^1 \in [-v_d * c_{i,j}^1, v_d * c_{i,j}^1]$.

184

185

186

In third step, each PS_j^1 is evaluated in battery model, and for the next step, different error ϵPS_j^1 is calculated for charging/discharging operation mode for both system signals, battery Voltage and battery SOC, in first place, the battery voltage error $\epsilon_v PS_j^1$ is calculated as:

$$\epsilon_v PS_j^k = (\epsilon Vc + \epsilon Vdc) / 2 \quad (7)$$

187

188

where, ϵVc and ϵVdc are the battery voltage error (charging/discharging). The mean errors are calculates as:

$$\varepsilon V_c = \frac{1}{j_c} \left(\sum_{i=1}^{j_c} \frac{|V_{c_m} - V_{c_s}|}{V_{c_m}} \right) \quad \text{and} \quad \varepsilon V_{dc} = \frac{1}{j_{dc}} \left(\sum_{i=1}^{j_{dc}} \frac{|V_{dc_m} - V_{dc_s}|}{V_{dc_m}} \right) \quad (8)$$

189 where V_m and V_s are the measured and simulated battery voltage respectively, and j is number
190 of samples. In similar way, the battery SOC error $\varepsilon_{SOC}PS_j^k$ is calculated as:

$$\varepsilon_{SOC}PS_j^k = (\varepsilon_{SOCc} + \varepsilon_{SOCdc}) / 2 \quad (9)$$

191 where, ε_{SOCc} and ε_{SOCdc} are the battery voltage error (charging/discharging). The mean
192 errors are calculates as:

$$\varepsilon_{SOCc} = \frac{1}{j_c} \left(\sum_{i=1}^{j_c} \frac{|SOC_{c_m} - SOC_{c_s}|}{SOC_{c_m}} \right) \quad \text{and} \quad \varepsilon_{SOCdc} = \frac{1}{j_{dc}} \left(\sum_{i=1}^{j_{dc}} \frac{|SOC_{dc_m} - SOC_{dc_s}|}{SOC_{dc_m}} \right) \quad (10)$$

193 where SOC_m and SOC_s are the measured and simulated battery SOC respectively, and j is
194 number of samples.

195
196 The goal is to minimize both εPS_j^k . The optimization process ends when a stop condition is met.
197 If the stop condition is not fulfilled, the GA creates a new population PS^{k+1} . This new population is
198 evaluated again. Therefore, at each step k , the system runs the model j times. Each time the systems
199 uses a row of PS^k . Simulation results are compared with real data so there is a simulation error for
200 each PS. This error is used to generate the next population to be tested or to decide if it is small
201 enough to finish the process. The stop condition is usually defined as a threshold for the minimum
202 εPS_j^k or as a maximum number of iterations.

203 Each GA uses a particular policy to create the new population from the previous evaluated one.
204 The goal is to converge to the optimal solution in a minimum number of steps. In order to perform
205 this operation, GAs includes random components to search for the global best solution which
206 include values of dispersion to spread or to focus the offspring near a possible solution. The model
207 parameters identification were set with an initial dispersions values between [-5, 5] from the initial
208 value.

209 4.1. GAs description

210 The PSO algorithm is a GA that emulates the behavior of a swarm in the action of the crop [28].
211 The swarm moves around a particle that finds a possible good place (solution) and explores this
212 location; if another particle finds a better solution, the swarm moves to this new place. The
213 advantages of PSO include the gradual reduction of the movement distance at each step (ω) to focus
214 the research on a small area and the capacity to keep the better solution found at each step in the
215 swarm memory (P_{best}) and the best solution of overall process (G_{best}). The algorithm uses two
216 coefficients in order to modulate the influence of P_{best} and G_{best} in the new swarm step (iteration).

217 On the other hand, one of the most recent published GA is CS [38]–[40], that emulates the
218 behavior of cuckoo birds related to their aggressive strategy of reproduction that colonize and
219 parasite the nests of another bird. The cuckoo chooses a nest with eggs, leaves its own egg; if the
220 egg is accepted and hatches, the brood will be fed by foster's birds. In CS, the probability that the
221 egg be found out and rejected is configurable as $Pa \in [0, 1]$. The CS movement strategy follows the
222 Lévy flights; each step has a random distance and an angular movement conditioned by
223 configurable values: α ($\alpha > 0$), and λ ($\lambda \in [1, 3]$).

224 4.2. New proposal

225 One important feature of PSO is its ability to gradually focus the search around the local
226 minimum. However, when the algorithm falls around a local minimum it is difficult to get a better
227 solution. This paper proposes the introduction of periodic perturbations inside the population in
228 order to force PSO reactivation. The perturbation will consist of a new population PS_j^l based on the
229 best global solution.

$$PS_j^l = \{c_{1,j}^l, c_{2,j}^l, c_{3,j}^l, \dots, c_{i,j}^l\}$$

$$c_{i,j}^l = (c_i^{GBest} \cdot z \cdot n) + c_i^{GBest} \quad (11)$$

230 where c_i^{GBest} is coefficient belonging to G_{Best} until iteration $l-1$, and n is perturbation value.
 231 Because the use of perturbations this proposal is named PSO+P. The perturbation is introduced into
 232 iteration around the stabilization of PSO, and then is necessary run first the PSO.

233 4.3. Algorithms configuration criteria

234 Different criteria currently exist for the algorithms configuration. This paper works with the
 235 more common configuration [28], [41], [46], [47] as it is shown in Table 3. Population size (j),
 236 iterations number (k) and initial dispersion (v_d) take equal values in all the algorithms.

237 **Table 3.** Genetic algorithms configuration.

Criteria	PSO	PSO+P	CS
Population size (j)	1000	1000	1000
Iterations (k)	100	100	100
Weight initial (ω_1)	0.9	0.9	-
Weight final (ω_2)	0.1	0.1	-
c_1	1	1	-
c_2	1	1	-
v_d	5	5	5
Iteration to perturb	-	10	-
Pa	-	-	0.5
α	-	-	1
λ	-	-	2

238

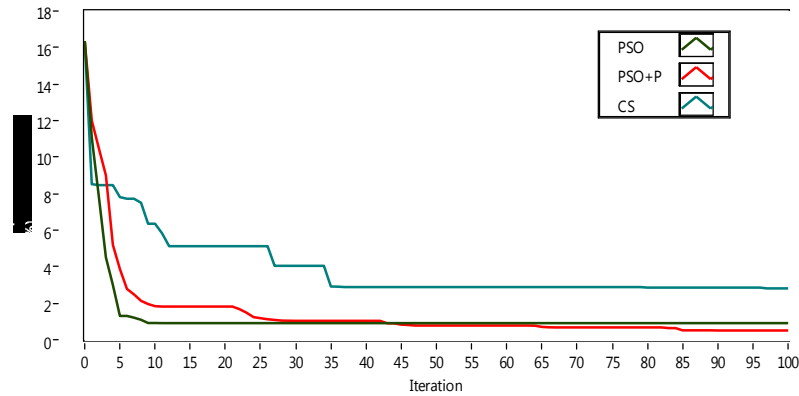
239 5. Results and discussion

240 5.1. Optimization results

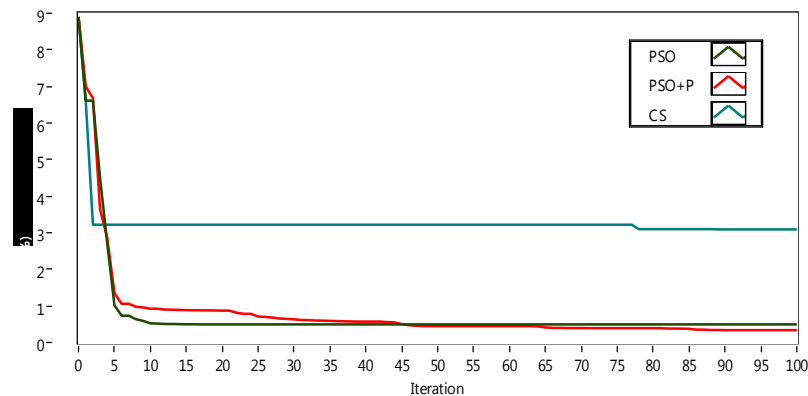
241 The model duality allows the use of different errors for both battery operation modes
 242 (charging/discharging). Therefore, we can study separately each behavior. Figure 5 shows both. In
 243 the charge mode, the CS does not find an optimal value of error and its last change takes place near
 244 80th iteration. PSO and PSO+P achieve similar error values. Despite PSO presents a fast search, it
 245 presents an early jam around a non-optimal solution. On the other hand, the perturbation feature of
 246 PSO+P lets it make a wide search and obtaining better results than previous GAs.

247

248 Related to discharge mode, the GAs performance shown similar performances as in charge
 249 mode. CS presents a more dynamic behaviour that obtains stabilization in iteration 36th, but with
 250 non-adequate optimization value. The fastest algorithm is PSO, which reaches an acceptable value
 251 less than 1.0% around the 10th iteration. PSO+P show a slightly slower behavior, but it obtains
 252 better results from the 43rd iteration onwards.



(a)



(b)

253 **Figure 5.** Optimization algorithms. (a) shows the algorithm performance in charge mode for a mean
 254 battery voltage, and (b) shows the discharge mode algorithm performance.

255 Results discard CS as a suitable method to fit the battery behavior. Therefore, only PSO and
 256 PSO+P need a closer look in order to select the best algorithm. A fast analysis over the curves shows
 257 that PSO is the faster algorithm but it falls in local minima so it loses search ability, thus confirming
 258 its known limitations. PSO+P obtain the best results but it requires more iterations to achieve it. A
 259 quantitative comparison is shown in Table 4. Criteria used to evaluate each algorithm are precision,
 260 velocity and computational cost. First, precision value is measured as the lowest error value reached
 261 by a GA. Second, the optimization speed is measured with the iteration when the algorithm makes
 262 its last improving. At last, computational cost is measured as the average time used by the computer
 263 to make single optimization iteration. Scores are calculated in each operation mode
 264 (charging/discharging) through the ratio between the obtained value by the algorithm and the
 265 lowest value achieved by algorithm. Therefore, a value of 1.00 represents the best result and a value
 266 of 2,000 stands for a 100% deviation from the best result. The algorithms ran under a PC with Intel
 267 core i5-3200, 31.GHz, 8 GB RAM and operating system W7-64 bits.

268

269 **Table 4.** Algorithms Comparison using the minimal mean error reached. d*= discharge mode; c*=
 270 Charge mode.
 271

Criteria/Algorithm		PSO		PSO+P		Cuckoo	
		d*	c*	d*	c*	d*	c*
Precision (error)	Value	0.50	0.91	0.34	0.51	3.09	2.81
	Score	1.48	1.78	1.00	1.00	9.23	5.53
Velocity (iteration)	Value	17.00	11.00	91.00	90.00	89.00	97.00
	Score	1.00	1.00	5.35	8.18	5.24	8.82
Computational cost (ms/iteration)	Value	0.41	0.41	0.42	0.42	0.71	0.71
	Score	1.00	1.00	1.03	1.03	1.72	1.72

272

273

274 5.2. Model performance and validation

275 Data in Table 4 describes PSO as the best algorithm regarding velocity and computational cost.
 276 However, PSO+P show the most accurate fit. Therefore, the model is fit from PSO+P results. These
 277 parameters are shown in Table 5.

278 **Table 5.** Parameters from PSO+P identification in daily data files.

Discharge		Charge	
V_{bdc} (V)	2.3003	V_{boc} (V)	2.2823
K_{bdc} (V)	0.1898	K_{boc} (V)	1.0227
P_{1dc} (VAh)	20.4751	P_{1c} (VAh)	2.4048
P_{2dc}	0.9282	P_{2c}	1.1928
P_{3dc} (Vh)	0.1481	P_{3c} (Vh)	0.0061
P_{4dc}	2.3350	P_{4c}	0.0285
P_{5dc} (Vh)	0.0362	P_{5c} (Vh)	0.0054
α_{rdc} ($^{\circ}\text{C}^{-1}$)	0.0365	α_{rc} ($^{\circ}\text{C}^{-1}$)	0.1008
k_{Idc}^*	2.2087	k_{Ic}^*	0.3254
$k_{c_batdc}^*$	2.5517	$k_{c_batc}^*$	0.3603
k_{socdc}^*	2.5509	k_{socc}^*	16.7918
k_{c120dc}^*	0.0470	k_{c120c}^*	0.3097

279

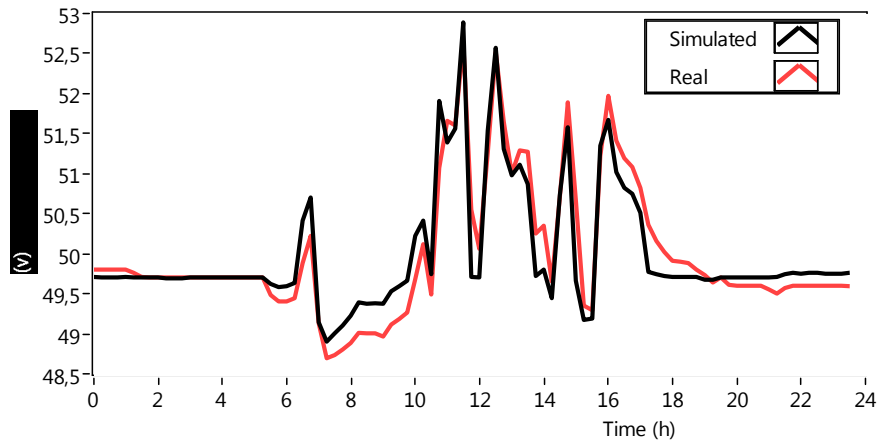
280

281

282

283

Figure 6 shows the results of the identification process with PSO+P. The simulated plot follows with high accuracy the real plot in battery voltage. The battery model with new extracted parameters presents a good matching with the reals measurement obtained from the research center.



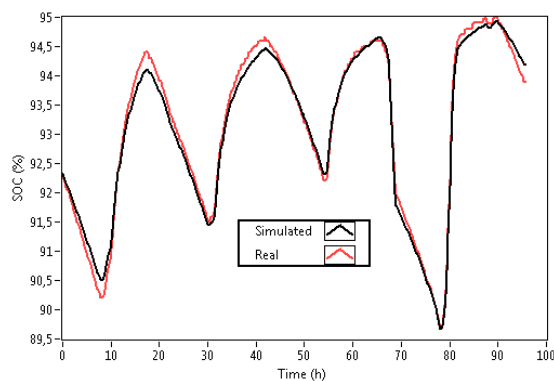
284
285

Figure 6. Simulation using identified parameters by PSO+P algorithm with one day data files.

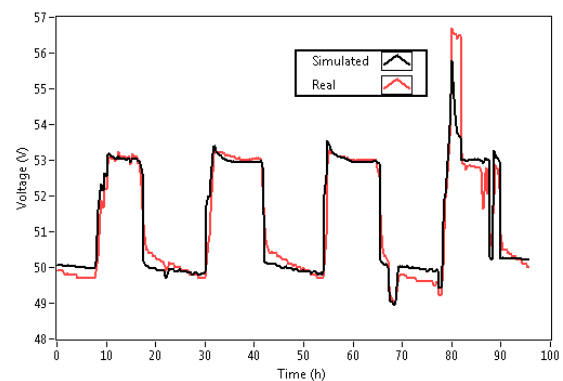
286 The simulation using the identification of parameters with PSO+P significantly improved the
287 mean errors presented in Table 2. The mean errors achieved with this method were 0.29% and 0.44%
288 for the battery voltage signal (discharging/charging, respectively) for an average between the two
289 signals of 0.365%.
290

291 5.3. Experimental validation

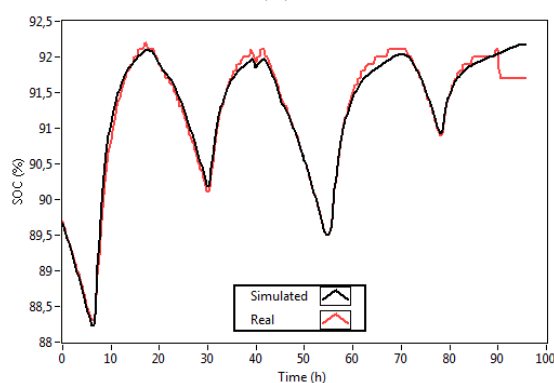
292 Model validation is carried out with data from three months divided into 4-day packages to be
293 compared with the results presented in [35]–[37]. In order to validate the developed model under
294 real conditions, this paper uses the parameters shown in Table 5. Figure 7 shows the results of the
295 experimental validation of several data packages for different months; left side shows the simulation
296 of SOC and right side presents the Voltage signal.
297



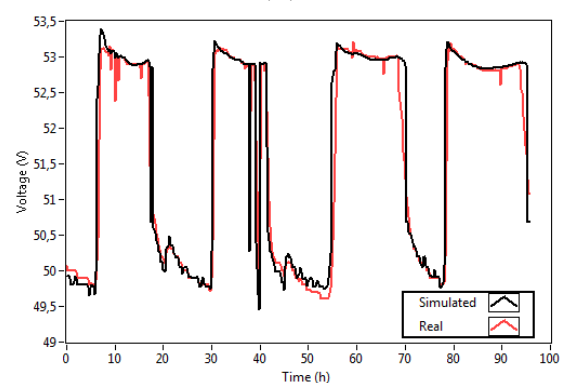
1(a)



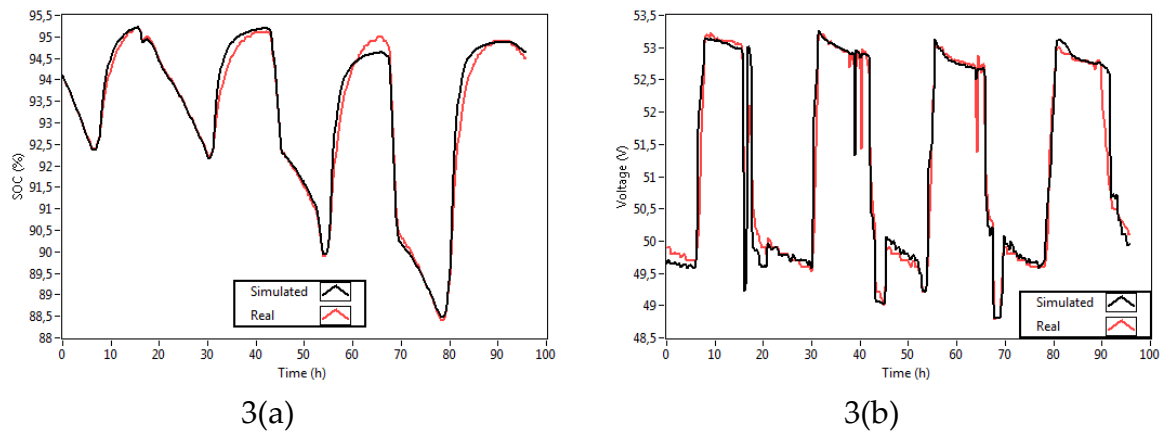
1(b)



2(a)



2(b)



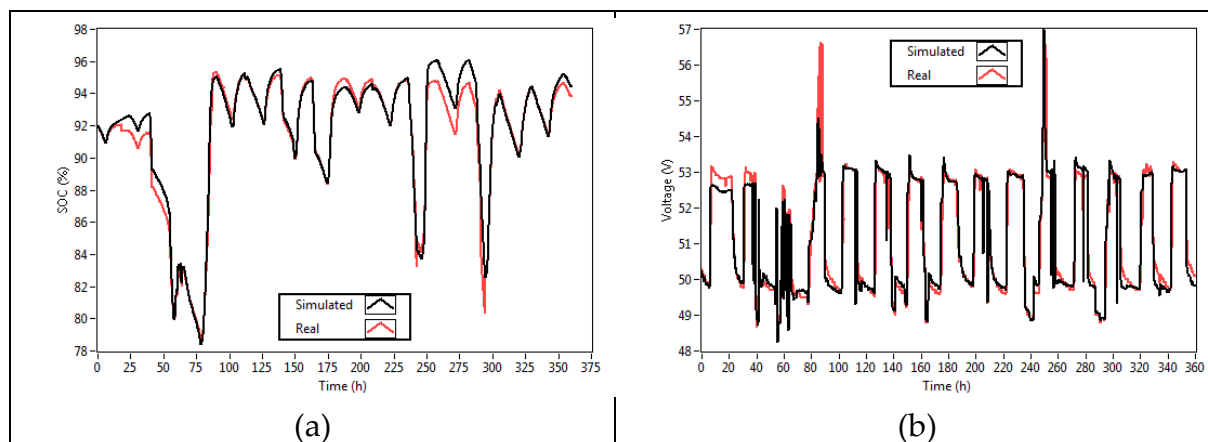
298 **Figure 7.** Battery voltage measurements (red plot) and simulation (black plot) results obtained by
 299 PSO+P algorithm identified parameters. 1-3(a) represents the Battery SOC signal; 1-3(b) represent the
 300 Battery Voltage Signals.

301 Validations 1 to 3 show that the model is able to follow the dynamics of the battery, despite in
 302 some cases it presents possible mistakes reading in the signal which may be due to of the
 303 measurement equipment. Those errors are shown as vertical falls and peaks without physic
 304 explanation due the reading period of 15 minutes. The mean error of each simulation regard to
 305 measured voltage is shown in Table 6.

306 **Table 6.** Mean error simulated vs measured voltage for 4-day package.

Signal	SOC			Voltage		
	Simulation	(a)	(b)	(c)	(a)	(b)
Charge Mode Error (%)	0.0606	0.0827	0.1787	0.2163	0.2504	0.2446
Discharge Mode error (%)	0.1223	0.1335	0.1383	0.3824	0.3347	0.5242
Mean	0.0956	0.1076	0.1602	0.3075	0.2904	0.3582

307 When the battery model is validated for a 15-day package with the parameters shown in Table 5
 308 the SOC mean error was 0.46% and voltage mean error 0.45% (see Figure 8). Again the model
 309 presents a good matching with the measured signal. However, on day 4th and 11th overcharging
 310 events occurred, and the model only was able to represent the second event.
 311
 312



313 **Figure 8** Battery voltage measurements and simulation results obtained by PSO+P algorithm for 15
 314 days. (a) represents the Battery SOC signal; (b) represents the Battery Voltage Signals.

315

316 6. Conclusions

317 The battery model proposed by Copetti has a good performance to represent battery dynamics.
318 However, when tested with real measurements, this model presents problems of scaling and delay
319 in the signal, so this paper have propose the inclusion of four new parameters to improve its
320 modelling capabilities. Despite, the Battery voltage equation includes the SOC equation, and the
321 battery voltage simulation result shows the SOC results in an implicit way, get the SOC simulation
322 results separately lets the model more useful for condition monitoring and the BBES management.
323

324 The model has been fit to represent the real behavior of a BESS placed at “El Chocó”. Colombia.
325 Despite, improvements should be made to the model. The complexity of the model implies the use
326 of GA to perform the optimization, so this paper has tested three GA in order to find the best
327 approach. Besides some well-known algorithms like CS and PSO, a new proposed algorithm
328 (Particle Swarm Optimization+Perturbation) have been used to identify and extract the parameters
329 of the lead acid OPzS type battery. The inclusion of the disturbance makes PSO+P more accurate
330 than PSO.
331

332 The present proposal has the ability to find *PS* to fit the model no matter the start point from
333 however, to continue the present work is necessary to make a sensibility analysis of the parameters
334 to define the influence of each parameter in the simulation results, and establish its adequate
335 boundaries
336

337 The battery model with the new extracted parameters presents a good matching with the reals
338 measurement obtained from the research center. The main advantage of the developed model is its
339 low computational cost and its ability to absorb reading problems, and scaling errors when the
340 simulation is valid with real measurements. The model and its fitting approach presented in this
341 paper may be applied to other types of batteries especially those used in stand-alone systems.
342

343 The battery model will be used to make a better battery energy management system from
344 research center placed at “El Chocó”. Colombia.
345

346 **Author Contributions:** The present work was developed with following contributions: Conceptualization,
347 methodology, software, validation, formal analysis, investigation and writing-original draft preparation and
348 data curation, H.E.A; E.B. and A.C.; Writing-review & editing, and supervision Á. P-N. and F.M.

349 **Funding:** This research was supported by “Implementación de un programa de desarrollo e investigación de
350 energías renovables en el departamento del chocó - BPIN:20130000100285; COLCIENCIAS (Administrative
351 department of science, technology and innovation of Colombia) scholarship program PDBCEX, COLDOC 586,
352 and the support provided by the Corporación Universitaria Comfauca, Popayán-Colombia.

353 **Conflicts of Interest:** Authors declare no conflict of interest. The founding sponsors had no role in the design of
354 the study; in the collection, analyses, or interpretation of data; in the writing of the manuscript, and in the
355 decision to publish the results.

356 References

- 357 1. [1] F. Díaz-González. A. Sumper. O. Gomis-Bellmunt. and R. Villafáfila-Robles. ‘A review of energy
358 storage technologies for wind power applications’. *Renew. Sustain. Energy Rev.*. vol. 16. no. 4. pp. 2154–
359 2171. 2012.
- 360 2. [2] A. Evans. V. Strezov. and T. J. Evans. ‘Assessment of utility energy storage options for increased
361 renewable energy penetration’. *Renew. Sustain. Energy Rev.*. vol. 16. no. 6. pp. 4141–4147. 2012.
- 362 3. [3] H. L. Ferreira. R. Garde. G. Fulli. W. Kling. and J. P. Lopes. ‘Characterisation of electrical energy
363 storage technologies’. *Energy*. vol. 53. pp. 288–298. 2013.

- 364 4. [4] S. Koochi-Kamali, V. V. Tyagi, N. A. Rahim, N. L. Panwar, and H. Mokhlis. 'Emergence of energy
365 storage technologies as the solution for reliable operation of smart power systems: A review'. *Renew.
366 Sustain. Energy Rev.*, vol. 25, pp. 135–165. 2013.
- 367 5. [5] T. Kousksou, P. Bruel, A. Jamil, T. El Rhafiki, and Y. Zeraoui. 'Energy storage: Applications and
368 challenges'. *Sol. Energy Mater. Sol. Cells*, vol. 120, pp. 59–80. 2014.
- 369 6. [6] R. Kaiser. 'Optimized battery-management system to improve storage lifetime in renewable energy
370 systems'. *J. Power Sources*, vol. 168, no. 1, pp. 58–65. 2007.
- 371 7. [7] A. Sayigh. *Renewable Energy in the Service of Mankind Vol I: Selected Topics from the World
372 Renewable Energy Congress WREC 2014*. Springer, 2015.
- 373 8. [8] S. Armstrong, M. E. Glavin, and W. G. Hurley. 'Comparison of battery charging algorithms for stand
374 alone photovoltaic systems'. *Power Electron. Spec. Conf. 2008 PESC 2008 IEEE*, pp. 1469–1475. 2008.
- 375 9. [9] Y. Yin, X. Luo, S. Guo, Z. Zhou, and J. Wang. 'A battery charging control strategy for renewable
376 energy generation systems'. *Proc. World Congr. Eng.*, vol. 1, pp. 2–4. 2008.
- 377 10. [10] R. Saiju and S. Heier. 'Performance analysis of lead acid battery model for hybrid power system'. in
378 *Transmission and Distribution Conference and Exposition. 2008. T&D. IEEE/PES. 2008*, pp. 1–6.
- 379 11. [11] K. M. Tsang, W. L. Chan, Y. K. Wong, and L. Sun. 'Lithium-ion battery models for computer
380 simulation'. in *Automation and Logistics (ICAL), 2010 IEEE International Conference on*, 2010, pp. 98–102.
- 381 12. [12] M. Nikdel. 'Various battery models for various simulation studies and applications'. *Renew. Sustain.
382 Energy Rev.*, vol. 32, pp. 477–485. 2014.
- 383 13. [13] W. H. Zhu, Y. Zhu, and B. J. Tatarchuk. 'A simplified equivalent circuit model for simulation of
384 Pb-acid batteries at load for energy storage application'. *Energy Convers. Manag.*, vol. 52, no. 8, pp. 2794–
385 2799. 2011.
- 386 14. [14] D. Fendri and M. Chaabene. 'Dynamic model to follow the state of charge of a lead-acid battery
387 connected to photovoltaic panel'. *Energy Convers. Manag.*, vol. 64, pp. 587–593. 2012.
- 388 15. [15] E. Hittinger, T. Wiley, J. Kluza, and J. Whitacre. 'Evaluating the value of batteries in microgrid
389 electricity systems using an improved Energy Systems Model'. *Energy Convers. Manag.*, vol. 89, pp. 458–
390 472. 2015.
- 391 16. [16] A. B. Ansari, V. Esfahanian, and F. Torabi. 'Discharge, rest and charge simulation of lead-acid
392 batteries using an efficient reduced order model based on proper orthogonal decomposition'. *Appl.
393 Energy*, vol. 173, pp. 152–167. 2016.
- 394 17. [17] N. Achaibou, M. Haddadi, and A. Malek. 'Modeling of lead acid batteries in PV systems'. *Energy
395 Procedia*, vol. 18, pp. 538–544. 2012.
- 396 18. [18] N. Achaibou, M. Haddadi, and A. Malek. 'Lead acid batteries simulation including experimental
397 validation'. *J. Power Sources*, vol. 185, no. 2, pp. 1484–1491. 2008.
- 398 19. [19] L. Devarakonda and T. Hu. 'Algebraic method for parameter identification of circuit models for
399 batteries under non-zero initial condition'. *J. Power Sources*, vol. 268, no. November 2014, pp. 928–940.
400 2014.
- 401 20. [20] A. Selmani, M. Outanoute, A. Lachhab, M. Guerbaoui, and B. Bouchikhi. 'Performance Evaluation of
402 Modelling and Simulation of Lead Acid Batteries for Photovoltaic Applications'. vol. 7, no. 2. 2016.
- 403 21. [21] K. Thirugnanam, E. R. J. TP, M. Singh, and P. Kumar. 'Mathematical modeling of Li-ion battery using
404 genetic algorithm approach for V2G applications'. *IEEE Trans. Energy Convers.*, vol. 29, no. 2, pp. 332–343.
405 2014.
- 406 22. [22] Z. Chen, C. C. Mi, Y. Fu, J. Xu, and X. Gong. 'Online battery state of health estimation based on
407 Genetic Algorithm for electric and hybrid vehicle applications'. *J. Power Sources*, vol. 240, pp. 184–192.
408 Oct. 2013.
- 409 23. [23] W. Liu, L. Liu, I.-Y. Chung, and D. A. Cartes. 'Real-time particle swarm optimization based
410 parameter identification applied to permanent magnet synchronous machine'. *Appl. Soft Comput.*, vol.
411 11, no. 2, pp. 2556–2564. 2011.
- 412 24. [24] L. Guo, Z. Meng, Y. Sun, and L. Wang. 'Parameter identification and sensitivity analysis of solar cell
413 models with cat swarm optimization algorithm'. *Energy Convers. Manag.*, vol. 108, pp. 520–528. 2016.
- 414 25. [25] E. K. Nyarko and R. Scitovski. 'Solving the parameter identification problem of mathematical models
415 using genetic algorithms'. *Appl. Math. Comput.*, vol. 153, no. 3, pp. 651–658. 2004.

- 416 26. [26] P. García-Triviño, A. J. Gil-Mena, F. Llorens-Iborra, C. A. García-Vázquez, L. M. Fernández-Ramírez,
417 and F. Jurado. 'Power control based on particle swarm optimization of grid-connected inverter for hybrid
418 renewable energy system'. *Energy Convers. Manag.*, vol. 91, pp. 83–92, 2015.
- 419 27. [27] M. D. A. Al-Falahi, S. D. G. Jayasinghe, and H. Enshaei. 'A review on recent size optimization
420 methodologies for standalone solar and wind hybrid renewable energy system'. *Energy Convers. Manag.*,
421 vol. 143, pp. 252–274, 2017.
- 422 28. [28] M. A. Rahman, S. Anwar, and A. Izadian. 'Electrochemical model parameter identification of a
423 lithium-ion battery using particle swarm optimization method'. *J. Power Sources*, vol. 307, pp. 86–97, 2016.
- 424 29. [29] X. Hu, S. Li, and H. Peng. 'A comparative study of equivalent circuit models for Li-ion batteries'. *J.*
425 *Power Sources*, vol. 198, pp. 359–367, 2012.
- 426 30. [30] A. Malik, Z. Zhang, and R. K. Agarwal. 'Extraction of battery parameters using a multi-objective
427 genetic algorithm with a non-linear circuit model'. *J. Power Sources*, vol. 259, pp. 76–86, 2014.
- 428 31. [31] J. Brand, Z. Zhang, and R. K. Agarwal. 'Extraction of battery parameters of the equivalent circuit
429 model using a multi-objective genetic algorithm'. *J. Power Sources*, vol. 247, pp. 729–737, 2014.
- 430 32. [32] L. Zhang, L. Wang, G. Hinds, C. Lyu, J. Zheng, and J. Li. 'Multi-objective optimization of lithium-ion
431 battery model using genetic algorithm approach'. *J. Power Sources*, vol. 270, pp. 367–378, 2014.
- 432 33. [33] D. Guasch and S. Silvestre. 'Dynamic battery model for photovoltaic applications'. *Prog. Photovolt.*
433 *Res. Appl.*, vol. 11, no. 3, pp. 193–206, 2003.
- 434 34. [34] J. B. Copetti, E. Lorenzo, and F. Chenlo. 'A general battery model for PV system simulation'. *Prog.*
435 *Photovolt. Res. Appl.*, vol. 1, no. 4, pp. 283–292, 1993.
- 436 35. [35] S. Blaifi, S. Moulahoum, I. Colak, and W. Merrouche. 'An enhanced dynamic model of battery using
437 genetic algorithm suitable for photovoltaic applications'. *Appl. Energy*, vol. 169, pp. 888–898, May 2016.
- 438 36. [36] S. Blaifi, S. Moulahoum, I. Colak, and W. Merrouche. 'Monitoring and enhanced dynamic modeling
439 of battery by genetic algorithm using LabVIEW applied in photovoltaic system'. *Electr. Eng.*, pp. 1–18,
440 2017.
- 441 37. [37] S. Blaifi, S. Moulahoum, N. Kabache, and I. Colak. 'An improved dynamic battery model suitable for
442 photovoltaic applications', in *Renewable Energy Research and Applications (ICRERA), 2015 International
443 Conference on*, 2015, pp. 694–698.
- 444 38. [38] X. S. Yang and S. Deb. 'Cuckoo Search via Levy flights'. in *2009 World Congress on Nature
445 Biologically Inspired Computing (NaBIC)*, 2009, pp. 210–214.
- 446 39. [39] S. Berrazouane and K. Mohammedi. 'Parameter optimization via cuckoo optimization algorithm of
447 fuzzy controller for energy management of a hybrid power system'. *Energy Convers. Manag.*, vol. 78, pp.
448 652–660, 2014.
- 449 40. [40] X.-S. Yang and S. Deb. 'Engineering optimisation by cuckoo search'. *Int. J. Math. Model. Numer.*
450 *Optim.*, vol. 1, no. 4, pp. 330–343, 2010.
- 451 41. [41] A. H. Gandomi, X.-S. Yang, and A. H. Alavi. 'Cuckoo search algorithm: a metaheuristic approach to
452 solve structural optimization problems'. *Eng. Comput.*, vol. 29, no. 1, pp. 17–35, Jan. 2013.
- 453 42. [42] I. Fister Jr., X.-S. Yang, I. Fister, J. Brest, and D. Fister. 'A Brief Review of Nature-Inspired Algorithms
454 for Optimization'. *ArXiv13074186 Cs*, Jul. 2013.
- 455 43. [43] C. Burgos, D. Sáez, M. E. Orchard, and R. Cárdenas. 'Fuzzy modelling for the state-of-charge
456 estimation of lead-acid batteries'. *J. Power Sources*, vol. 274, pp. 355–366, 2015.
- 457 44. [44] H. L. Chan. 'A new battery model for use with battery energy storage systems and electric vehicles
458 power systems'. *2000 IEEE Power Eng. Soc. Winter Meet. Conf. Proc. Cat No00CH37077*, vol. 1, no. c, pp.
459 470–475, 2000.
- 460 45. [45] A. Szumanowski and Y. Chang. 'Battery management system based on battery nonlinear dynamics
461 modeling'. *IEEE Trans. Veh. Technol.*, vol. 57, no. 3, pp. 1425–1432, 2008.
- 462 46. [46] Q. Li, W. Chen, Y. Wang, S. Liu, and J. Jia. 'Parameter Identification for PEM Fuel-Cell Mechanism
463 Model Based on Effective Informed Adaptive Particle Swarm Optimization'. *IEEE Trans. Ind. Electron.*,
464 vol. 58, no. 6, pp. 2410–2419, Jun. 2011.
- 465 47. [47] M. Ye, X. Wang, and Y. Xu. 'Parameter identification for proton exchange membrane fuel cell model
466 using particle swarm optimization'. *Int. J. Hydrog. Energy*, vol. 34, no. 2, pp. 981–989, 2009.
- 467